Appl Biochem Biotechnol
DOI 10.1007/s12010-015-1579-1

An Organophosphorus Hydrolase-Based Biosensor for Direct Detection of Paraoxon Using Silica-Coated Magnetic Nanoparticles

Reza Khaksarinejad[1] · **Afshin Mohsenifar**[2,3] · **Tavoos Rahmani-Cherati**[2] · **Rezvan Karami**[1] · **Meisam Tabatabaei**[3,4]

Received: 2 December 2014 / Accepted: 12 March 2015

Abstract Rapid detection of organophosphorous (OP) compounds such as paraoxon would allow taking immediate decision on efficient decontamination procedures and could prevent further damage and potential casualties. In the present study, a biosensor based on nanomagnet-silica core-shell conjugated to organophosphorous hydrolase (OPH) enzyme was designed for detection of paraoxon. Coumarin1, a competitive inhibitor of the OPH enzyme, was used as a fluorescence-generating molecule. Upon excitation of cumarin1 located at the active site of the enzyme, i.e., OPH, the emitted radiations were intensified due to the mirroring effect of the nanomagnet-silica core-shell conjugated to the enzyme. In presence of paraoxon and consequent competition with the fluorophore in occupying enzyme's active site, a significant reduction in emitted radiations was observed. This reduction was proportional to paraoxon concentration in the sample. The method worked in the 10- to 250-nM concentration range had a low standard deviation (with a coefficient of variation (CV) of 6–10 %), and the detection limit was as low as 5×10^{-6} μM.

✉ Afshin Mohsenifar
mohsenifar_a@yahoo.com

✉ Meisam Tabatabaei
meisam_tab@yahoo.com

[1] Department of Toxicology, Faculty of Medical Sciences, Tarbiat Modares University, Tehran, Iran

[2] Research & Development Department, Nanozino Co., Tehran, Iran

[3] Nanobiosensor Research Group, Nanosystems Research Team (NRTeam), Karaj, Iran

[4] Microbial Biotechnology and Biosafety Department, Agricultural Biotechnology Research Institute of Iran (ABRII), AREEO, Karaj, Iran

Published online: 01 April 2015

Keywords Nanobiosensor · Organophosphorous hydrolase · Nanomagnet-silica core-shell · Paraoxon · Kinetics

Introduction

Organophosphorous (OP) compounds are widely used as pesticides, insecticides, and chemical warfare agents. Some members of this class are extremely toxic to mammals. Technically, these neurotoxins are powerful inhibitors of esterases, such as acetylcholinesterase (AChE) or butyrylcholinesterase (BChE) involved in nerve function [1]. OP is a naturally degradable compound; however, due to its heavy application in urban and rural areas, a considerable amount of OP residues could also be found in soil and water. Hence, accurate detection of even very low concentration of such compounds in the environment is of crucial importance.

Sensitive biosensors based on AChE or BChE inhibition have been developed for OP detection [2–5]. A number of other enzymes such as urease and glucose oxidase have also been also used in inhibition-based biosensors for OP neurotoxins [6, 7]. Basically, in the inhibition-based biosensors, the OP agents interact with the active site of the enzyme, resulting in loss of enzyme activity and hence a decrease in sensor signals. Moreover, a class of enzymes, namely, organophosphorous hydrolases (OPHs), has been increasingly used to develop biodetection systems for OPs. It is a homodimeric enzyme that can degrade a broad spectrum of organophosphorous pesticides such as paraoxon, parathion, coumaphos, and diazinon and has been first isolated from *Pseudomonas diminuta* MG and *Flavobacterium* sp. ATCC 27551 [8].

Immobilization of proteins, e.g., enzymes onto solid supports, has been found advantageous for a wide variety of biosensing [9]. Enzyme immobilization could lead to favorable or unfavorable physical and chemical changes in enzyme properties such as stability and activity [10]. In other words, some immobilization or entrapment methods could cause significant structural deformation of the enzyme, leading to reduced enzymatic activity or vice versa. Therefore, significant optimization of the immobilization method is often required [11, 12]. Chemical immobilization generally involves enzyme attachment to a matrix such as nanoparticles via cross-linking or covalent bonding. Moreover, surface modification of nanoparticles is one of the key technologies to achieve optimized immobilization of enzymes and consequently spread their applications. Among various nanoparticles, silver-silica core-shell was regarded promising for development of nanobiosensors due to its intensified fluorescence signals caused by the silica layer [13]. Furthermore, organic molecules such as enzymes could be attached to this silica layer via covalent [14] or hydrogen bonding [15] .

In this investigation, in an effort to further reduce the detection limit of an OPH-gold nanoparticle (AuNP) nanobiosensor previously reported by our team [16], OPH enzyme was immobilized on nanomangetic-silica core-shell (Fe_3O_4-silica NPs). The detection mechanism of this system was essentially based on the replacement of a competitive inhibitor of OPH, i.e., coumarin1 (a fluorophore, with a similar chemical structure to OP), by paraoxon and consequent change in fluorescence intensity. In fact, the silica layer would act as a diamond-like intensifier of the generated signals (Scheme 1). Finally, the performance of the developed OPH-(Fe_3O_4-silica NP) nanobiosensor was evaluated under different conditions such as pH, temperature, and solvents.

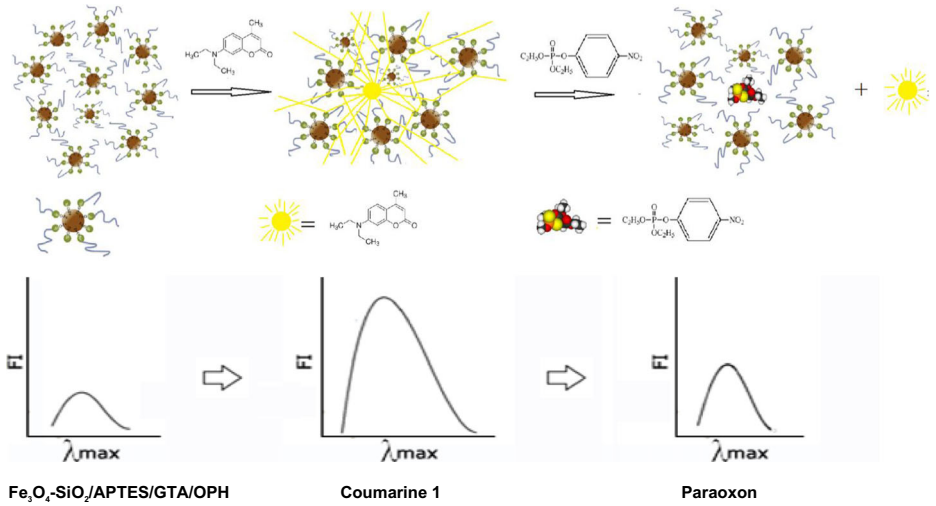

Scheme 1 Schematic presentation of the mechanism of the proposed Fe_3O_4-SiO_2/APTES/GTA/OPH nanobiosensor for the detection of paraoxon. The fluorescence intensity of the system increases and then decreases upon the conjugation of coumarine1 and paraoxon with the nanobiosensor, respectively

Material and Methods

OPH was extracted from *Pseudomonas diminuta* and purified as described by [16]. Paraoxon was purchased from Sigma-Aldrich (USA). Tetraethoxysilane (TEOS) and (3-aminopropyl)triethoxysilane (APTES) were obtained from Merck (Germany). All the solutions were prepared using redistilled water.

Synthesis of Fe_3O_4 NPs

Ten milliliters of NH_3 was added quickly into 50 ml of the prepared Fe(III)/Fe(II) solution (2:1 molar ratio, respectively), under vigorous stirring and N_2 purging [17]. pH was then adjusted to 9 and stirred for 1 h at room temperature. The prepared Fe_3O_4 NPs were then removed using a magnetic bar and washed with distilled water three times to remove un-reacted materials. The Fe_3O_4 NPs were then sonicated for 10 min in presence of 1.5 mM trisodium citrate solution as a stabilizer using a probe type Hielscher sonicator (Germany) (50 kHz, 0.5 cycle). Characteristics of NPs were investigated by TEM and SEM.

Synthesis of Fe_3O_4-SiO_2 Core-Shell

Twenty milligrams of Fe_3O_4 NPs was added into 1.5 mM trisodium citrate solution and ethanol (4:1) and was sonicated for 20 min; upon complete dispersion of the Fe_3O_4 NPs, 50 μl of NH_3 was added into the mixture and was stirred gently. Subsequently, 200 μl TEOS was added and stirred for 3 h followed by an addition of 10 μl APTES [18].

Preparation of Nanobioconjugate: Fe_3O_4-SiO_2/APTES/GTA/OPH

OPH enzyme was immobilized on APTES-activated silica surface of the Fe_3O_4-SiO_2 core-shell using glutaraldehyde (GTA) as cross-linker. The Fe_3O_4-SiO_2 core-shell solution was added to excess amount of GTA (100- to 1000-fold higher than the concentration of Fe_3O_4-SiO_2 core-shell) and was gently stirred for 12 h. Then, product was then washed with deionized water and centrifuged to remove un-reacted GTA. Fourier transform infrared (FTIR) was used to conform the attachment between Fe_3O_4-silica NPs and GTA. The Fe_3O_4-SiO_2 core-shell-GTA solution was then added to OPH enzyme in 0.4 mg dinitropyridine solution as a catalyst and was stirred slowly for 4 h. Then, 4 mg $NaBH_4$ was included into the solution for 1 h.

Paraoxon Detection and Nanobiosensor Evaluation

Fluorescence intensity (FI) of a 50-pmol solution of coumarin1 in Tris-HCl buffer (50 mM, pH 8.0) was recorded on a spectrofluorometer. The sample was then excited at 380 nm and emission spectrum was recorded in 400–600 nm. Excitation slit and emission slit were selected as 5 and 10 nm, respectively. Then, a 10-μl sample of the nanobioconjugate was added and emission of coumarin1 was recorded as mentioned above. Different concentrations of paraoxon solution (0, 10, 50, 100, 150, 200, and 250 nM) were prepared and then sequentially added to a solution containing coumarin1 as well as the nanobioconjugate in order to determine the detection limit. Emission spectrum of coumarin1 was also recorded at each concentration of paraoxon as a standard curve for estimation of paraoxon concentration in serum samples. Limit of detection (LOD) was measured based on the equation $LOD=3S_0\,K$, where S_0 is the standard deviation of blank measurements ($n=6$) and K is the slope of calibration curve [19, 20].

The performance of the developed Fe_3O_4-SiO_2/APTES/GTA/OPH nanobioconjugate was evaluated using real samples. More specifically, human sera were collected from healthy individuals living in OP-free regions and then treated with increasing concentrations of paraoxon solution (10 to 250 nM). The paraoxon-treated serum samples were then added to the reaction mixture containing coumarin1 and the nanobioconjugate, and the fluorescence intensity of coumarin1 was recorded for each serum sample as described above. Untreated serum samples were used as control or blank.

Kinetic Studies

Kinetics of free and nanoconjugated OPH were studied at different temperatures (30, 37, 40, 45, 50, 70, 90 °C) and pH (3–11 with 1 interval) and in presence of a number of solvents (methanol, 2-propanol, and ethanol). The activity of the free and nanoconjugated OPH was measured based on hydrolyzing rate of paraoxon as depicted in the following reaction:

$$\text{Paraoxon} \xrightarrow{\text{OPH}} \text{Diethyl phosphate} + p\text{-nitrophenol}$$

The change in absorbance of *p*-nitrophenol at 410 nm ($\varepsilon_{410}=16{,}500\ M^{-1}\ cm^{-1}$) was measured using a spectrophotometer (Shimadzu; UV-3100, Japan)

Results and Discussion

In the present study, OPH enzyme was immobilized on APTES-activated silica surface of the Fe_3O_4-SiO_2 core-shell using GTA as cross-linker. As there is a large number of hydroxyl functional groups on the silica surface, the attachment of enzyme NH_2 groups to the silica particles would not be feasible. Therefore, we activated the silica surface by using APTES. In fact, NH_2 groups were added onto the silica surface through the APTES-mediated activation procedure. Then, the enzyme's NH_2 groups and those already seated into silica surface were attached using GTA. Enzyme immobilization onto NPs by GTA linker has been shown to lead to higher enzymatic activity compared to free enzymes.

Confirmation of Fe_3O_4 NPs and Fe_3O_4-SiO_2 Core-Shell Synthesis

Figure 1 confirms the size and uniformity of the synthesized Fe_3O_4 NPs as examined by using TEM. The size of the NPs were measured in the range between 20 to 50 nm. Figure 2 presents the SEM micrograph (a) and TEM micrograph (b) of the synthesized Fe_3O_4-SiO_2 core-shells. The size of the core-shells was measured at 20 nm with the thickness of the shell estimated at 0.1 nm. As clearly observed, all the core-shells were uniform in size and shape. This could play an important role in intensifying the fluorescence consistently.

In fact, this study was inspired by that of [21], in which the authors used silver-silica core-shells to intensify the fluorescence. Replacing silver NPs by Fe_3O_4 NPs in the present study not only implies the possibility of using other metal NPs in order to achieve the same objective as that of [21], but also would offer additional advantages considering the unique features of Fe_3O_4 NPs, e.g., facilitated isolation of nanobioconjugates from a medium.

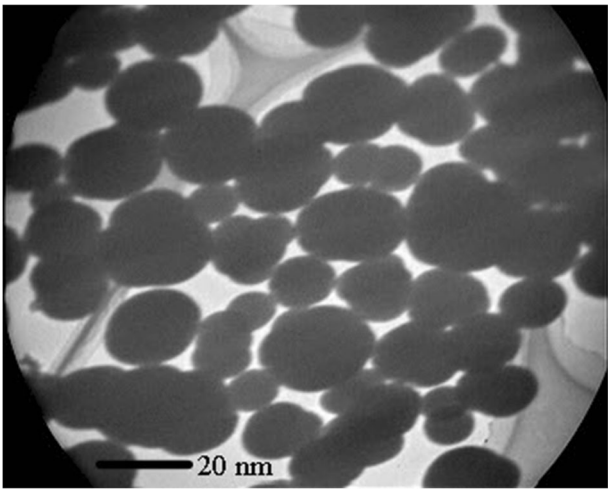

Fig. 1 TEM micrograph of the synthesized Fe_3O_4 NPs

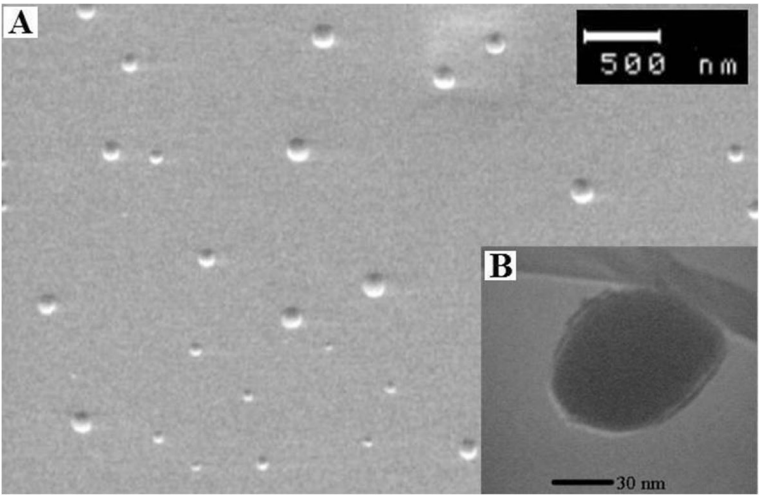

Fig. 2 **a** SEM and **b** TEM micrographs of the synthesized Fe_3O_4-SiO_2 core-shells

Conjugation of Fe_3O_4-SiO_2 Core-Shells and OPH

Successful production of Fe_3O_4-SiO_2/APTES/GTA/OPH nanobioconjugates was revealed by FTIR analysis as shown in Fig. 3. The C–H stretching observed at 2940 cm^{-1} represents the presence of GTA in the nanobioconjugates produced. However, since there is no peak at 1715 cm^{-1} region representing the GTA's carbonyl functional group, it could be concluded that a Schiff base bond was formed between GTA and the OPH enzyme.

Nanobiosensor Evaluation

As shown in Fig. 4a, maximum coumarin1 fluorescence intensity was observed at 470 nm. By addition of the nanobioconjugate to coumarin1, the fluorescence intensity increased significantly, revealing the intensifying impact of Fe_3O_4-SiO_2 core-shells on the fluorescence emission of coumarin1 (Fig. 4a). Subsequently, different concentrations of paraoxon (0, 10, 50, 100, 150, 200, and 250 nM) were added to the mixture of coumarin1-nanobioconjugate, and normalized fluorescence intensities were estimated. In fact, in presence of paraoxon, which has a high affinity for the active site of the OPH enzyme, coumarin1 with less affinity would simply leave the enzyme's active site. Therefore, even at the least concentration of paraoxon tested (10 nM), a noticeable reduction in the coumarin1 fluorescence intensity was achieved. Changes in coumarin1 fluorescence intensity were directly proportional to the final concentration of paraoxon in the solution (Fig. 4a, b). The linear changes in the fluorescence intensity of coumarin1 after the addition of different concentrations of paraoxon to nanobioconjugate could be described by the Eq. 1:

$$y = -2.2077x + 929.64 \left(R^2 = 0.9882\right) \quad (1)$$

where y is the fluorescence intensity and x is the concentration of paraoxon. The calibration curve developed was also used for estimation of paraoxon concentration in the real

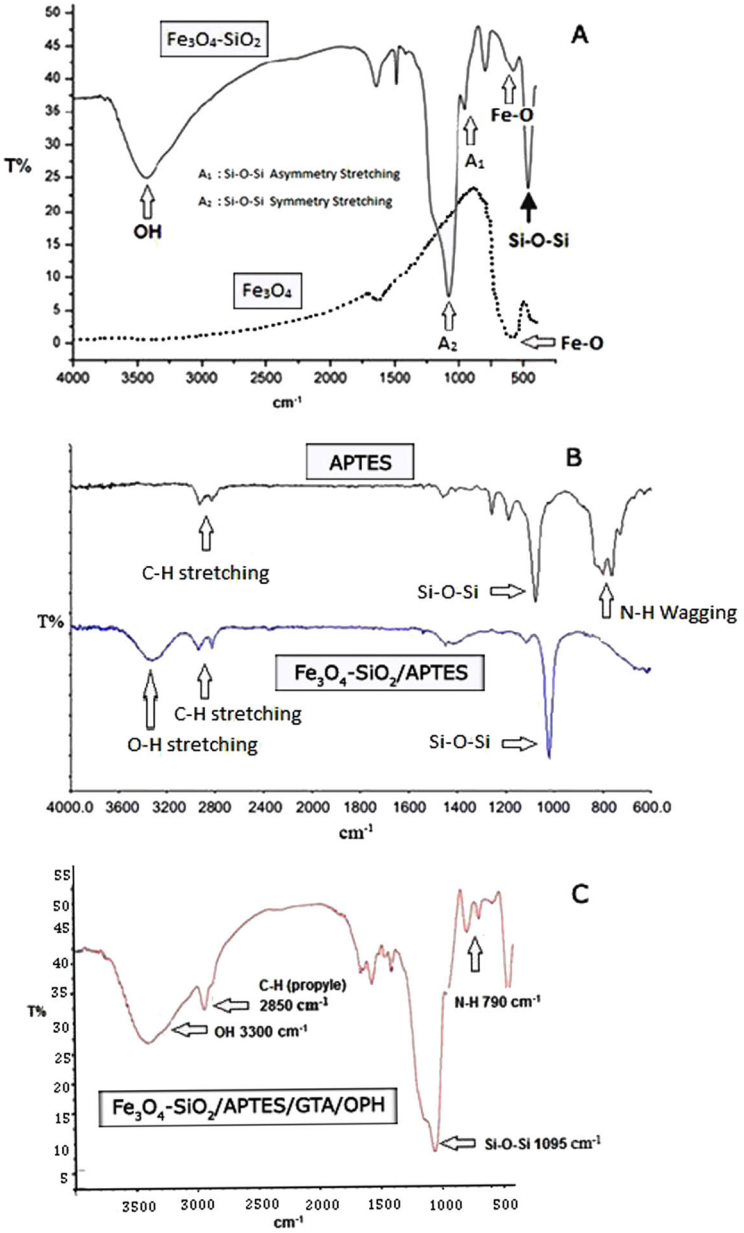

Fig. 3 FTIR spectrum of **a** Fe_3O_4 NPs and Fe_3O_4-SiO_2 core-shells, **b** APTES and Fe_3O_4-SiO_2/APTES, and **c** Fe_3O_4-SiO_2/APTES/GTA/OPH nanobioconjugate

serum samples. The results obtained are summarized in Table 1. The low coefficient of variation (CV) value achieved (6–10 %) confirmed the precision of the designed nano-biosensor in determination of paraoxon concentration in human sera. Additionally, low relative CV% (n=6) showed excellent data reproducibility. Moreover, it was revealed that naturally existing compounds in serum did not cause significant interferences in

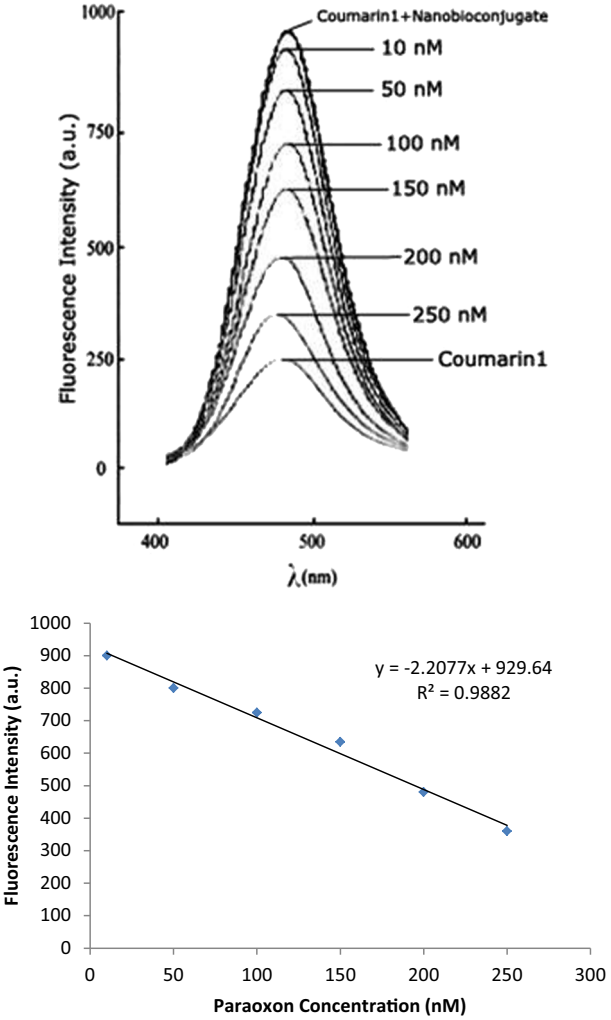

Fig. 4 **a** Changes in the fluorescence intensity of coumarin1 in the absence and the presence of different concentrations of paraoxon (0, 10, 50, 100, 150, 200, and 250 nM), and **b** the linear changes in the fluorescence intensity of coumarin1 after the addition of different concentrations of paraoxon to the nanobioconjugate used as the standard curve

determination of paraoxon by spectrofluorometer. Overall, the high sensitivity along with simple, direct determination as well as one-step protocol is the main advantages of the newly-designed nanobiosensor.

Limit of detection (LOD) was also measured at 5×10^{-6} μM, based on the equation explained earlier. Overall, the intensifying impact of the Fe_3O_4-SiO_2 core-shells on the fluorescence emission of coumarin1 played an important role in functionality of the developed nanobiosesor. This could explain the lower detection limit achieved using the

Table 1 The results of estimation of paraoxon concentration in human serum samples

Sample	Paraoxon conc. (real value; nM)	Paraoxon conc. (estimated value) Mean±SD	CV (%)
S1	10	11±0.5	10
S2	50	47±5	6.0
S3	100	107±7	7.0
S4	150	161±9	7.3
S5	200	218±22	9.0
S6	250	270±27	8.0

CV coefficient of variation

present nanobiosensor in comparison with those of the previous investigations (Table 2) [9, 16, 22–32].

As seen in the Table 2, in our previous study, the detection mechanism was based on the quenching properties of the AuNPs, and therefore, the maximal fluorescence intensity achieved was solely determined by the intrinsic fluorescence intensity of coumarin1. On the other hand, in the present study, the intrinsic intensity of coumarin1 was significantly magnified through the presence of the Fe_3O_4-SiO_2 core-shells. In fact, by enhancing the signal (e.g., the fluorescence intensity), sensitivity could be increased and lower detection limits could be achieved. On such basis and as a result of the magnified fluorescence intensity of coumarine1 in the present study, lower concentrations of paraoxon could be detected (Table 2).

Kinetic Studies

Figure 5 represents the comparison of the activity of the free OPH enzyme and its nanobioconjugate counterpart, i.e., Fe_3O_4-SiO_2 core-shell-OPH under different conditions including pH (3–11) (Fig. 5a) and temperature (25–90 °C) (Fig. 5b) and in presence of a number of solvents (methanol, 2-propanol, and ethanol). The optimum pH and temperature values for both free and nanobioconjugated OPH to achieve the highest enzymatic activity were 8 and 37 °C, respectively. However, in comparison with free OPH, the Fe_3O_4-SiO_2 core-shell-OPH withstood wider pH (4–8) and temperature (>50 °C) ranges. Moreover, in terms of the enzyme resistance in presence of solvents, the nanobioconjugated enzyme performed significantly better when exposed to ethanol and maintained its activity almost intact at different solvent percentages tested. On the contrary, the activity of the free enzyme was reduced by half due to the increasing ethanol concentration up to 25 % in the environment (Fig. 5c). As for 2-propanol, the nanobioconjugated enzyme showed an overall better performance when compared to the free one, but both were negatively affected due to the chemical exposure. Nanobioconjugation did not seem to have improved OPH resistance to methanol as presented in Fig. 5d. This could be ascribed to strong solvency characteristics of methanol in comparison with the other two solvents tested. In other words, methanol possesses the smallest molecule among the investigated solvents and as a result is more capable of forming hydrogen bonds and consequently reducing enzymatic activity. Figure 6 shows the enzymatic kinetic parameters (K_m, V_{max}, and k_{cat}) for both free and nanobioconjugated enzyme. As seen, the nanobioconjugation procedure practiced significantly improved the kinetic parameters of the OPH enzyme.

Table 2 Comparison of OPH-based biosensors with the nanobiosensor developed in the present study

OP substrate	Enzyme used	Configuration	Method	LOD (μM)	Reference
Paraoxon Methyl parathion	OPH	OPH with a histidine tail (OPH_{6His}) bioconjugated with ryranine—with the aid of silica-coated silver nanoparticles	Optical (flourometric)	2×10^{-2} to 2×10^{-3} $5–1\times10^{-2}$	[22]
Paraoxon	OPH	*Escherichia coli* cells containing periplasmic-OPH onto the surface of a 96-well microplate using Mussel adhesive protein (MAP) as a microbial cell-immobilizing linker	Optical (microscopic)	5	[23]
Dichlofenthion	OPH HRP	OPH combined with horse radish peroxidase (HRP)	Electrochemical (amperometric)	24	[24]
Paraoxon	OPH	OPH-functionalized carbon nanotube (CNT)	Electrochemical (amperometric)	1×10^{-2}	[25]
Paraoxon Diazinon Malathion Coumaphos	OPH	Reversible inhibition of OPH by copper complexed meso-tri (4-sulfonato phenyl) mono(4-carboxy phenyl) porphyrin (CuC_1TPP)	Optical (spectrophotometric)	7×10^{-6} 8×10^{-4} 1×10^{-3} 2.5×10^{-4}	[26]
Paraoxon	OPH	Cross-linking OPH with bovine serum albumin and glutaraldehyde	Electrochemical (potentiometric)	2	[27]
Paraoxon	OPH	Fluorescein isothiocyanate covantly bound to OPH	Optical (flourometric)	8	[28]
Paraoxon Prathion	OPH	OPH immobilized on a nylon microporousmembrane by cross-linking with glutaraldehyde	Optical (spectrophotometric)	2 – 5	[29]
Paraoxon Methyl parathion	OPH	OPH deposited on the electrode in Nafion film	Electrochemical (amperometric)	9×10^{-2} 7×10^{-2}	[30]
Paraoxon Methyl parathion	OPH	OPH-modified carbon-paste working electrode, a Ag/AgCl reference electrode and a platinum wire counter electrode	Electrochemical (amperometric)	0.9 0.4	[31]
Fenitrothion Thiobenzenephosphonate	OPH	Genetically engineered *p*-nitrophenol-degrading *Pseudomonas putida* JS444 with surface-expressed organophosphorus hydrolase and modified carbon paste electrode as amperometric transducer	Electrochemical (amperometric)	$1.4–1.6\times10^{-3}$	[32]
Paraoxon	OPH	OPH-conjugated gold nanoparticles with 7-hydroxy-9H-(1,3-dichloro-9,9-dimethylacridin-2-one (DDAO phosphate) as decoy	Optical (flourometric)	20	[9]
Paraoxon	OPH	OPH-conjugated gold nanoparticles with and without linking system (glutaraldehyde-cystamine) and cumarin1 as decoy	Optical (flourometric)	5×10^{-5}	[16]
Paraxon	OPH	OPH-conjugated nanomagnet-silica core-shell with cumarin1 as decoy	Optical (flourometric)	5×10^{-6}	Present study

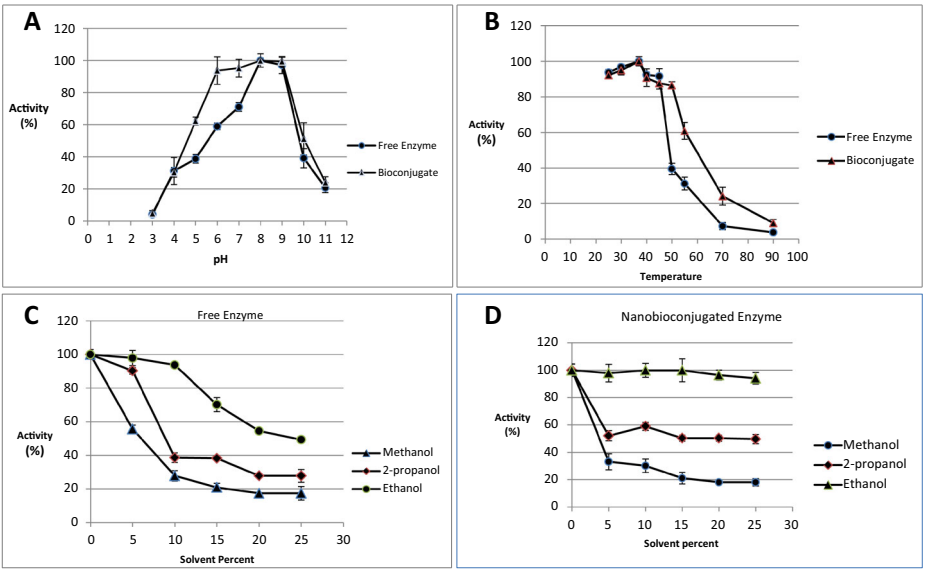

Fig. 5 Comparison of the activity of the free OPH enzyme and its nanobioconjugated counterpart at different **a** pH (3–11) and **b** temperatures (30, 37, 40, 45, 50, 70, 90 °C), and **c**, **d** under the influence of different solvents (methanol, 2-propanol, and ethanol)

Conclusion

A new spectrofluorometric OPH-based assay for accurate direct detection of paraoxon is described. Having compared the OPH-based biosensors reported elsewhere with the nanobiosensor developed in the present study, the enhancing role achieved herein was ascribed to the magnet-silica core-shell used. Moreover, in this study, the immobilization of the OPH enzyme on the Fe_3O_4 NPs was found to have improved the catalytic activity of the enzyme considerably under different conditions (i.e., pH, temperature, and solvent presence). As a whole, the low detection limit in order of 10^{-6} μM paraoxon, simple fabrication method, and analysis

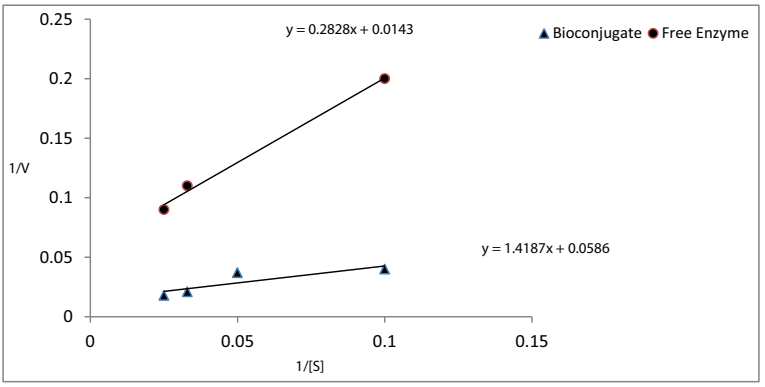

Fig. 6 The enzymatic kinetic parameters (K_m, V_{max}, and k_{cat}) of the free OPH enzyme and its nanobioconjugated counterpart

combined with the unique features of Fe_3O_4 NPs (e.g., facilitated isolation of nanobioconjugates from a medium) could introduce the present OPH-conjugated nanomagnet-silica core-shell (with Cumarin1 as decoy), as a strong tool for high-throughput detection of paraoxon.

Acknowledgments The authors would like to thank Nanozino Co. and Nanosystems Research Team (NRTeam) for financially supporting the present research.

Compliance with Ethical Standards The authors declare no conflict of interest. No ethical approval was required.

References

1. Du, D., Wang, M., Cai, J., & Zhang, A. (2010). Sensitive acetylcholinesterase biosensor based on assembly of β-cyclodextrins onto multiwall carbon nanotubes for detection of organophosphates pesticide. *Sensors Actuators B Chem, 8*, 337–341.
2. Du, D., Chen, A., Xie, Y., Zhang, A., & Lin, Y. (2011). Nanoparticle-based immunosensor with apoferritin templated metallic phosphate label for quantification of phosphorylated acetylcholinesterase. *Biosensors and Bioelectronics, 26*, 3857–3863.
3. Lu, D., Wang, J., Wang, L., Du, D., Timchalk, C., & Barry, R. (2011). A novel nanoparticle-based disposable electrochemical immunosensor for diagnosis of exposure to toxic organophosphorus agents. *Advanced Functional Materials, 21*, 4371–4378.
4. Susan, J., Dyk, V., & Pletschke, B. (2011). Review on the use of enzymes for the detection of organochlorine, organophosphate and carbamate pesticides in the environment. *Chemosphere, 82*, 291–307.
5. Pohanka, M. (2012). Acetylcholinesterase based dipsticks with indoxylacetate as a substrate for assay of organophosphates and carbamates. *Analytical Letters, 45*, 367–374.
6. Aragay, G., Pino, F., & Merkoçi, A. (2012). Nanomaterials for Sensing and Destroying Pesticides. *Chemical Research, 112*, 5317–5338.
7. Sassolas, A., Simón, B. P., & Marty, J. L. (2012). Biosensors for Pesticide Detection: New Trends. *American Journal of Analytical Chemistry, 3*, 210–232.
8. Mulbry, W. W., Karns, J. S., Kearney, P. C., Nelson, J. O., Mc Daniel, C. S., & Wild, J. R. (1986). Identification of a plasmid-borne parathion hydrolase gene from *Flavobacterium* sp. by southern hybridization with opd from *Pseudomonas diminuta. Applied and Environmental Microbiology, 51*, 929–930.
9. Simonian, A., Good, T., Wang, S., & Wild, J. (2005). Nanoparticle based optical biosenses for the direct detection of organophosphate chemical warfare agent and pesticides. *Analytica Chimica Acta, 534*, 69–77.
10. Calleri, E., Temporini, C., Massolini, G., Caccialanza, G., & Penicillin, G. (2004). Penicillin G acylasebased stationary phases. *Journal of Pharmaceutical and Biomedical Analysis, 35*, 243–258.
11. Chi-Fang, W., Hyung, J. C., James, J., & Bentley, E. (2002). GFP-visualized immobilized enzymes: Degradation of paraoxon via organophosphorus hydrolase in a packed column. *Biotechnology Bioengineering, 77*, 212–218.
12. Luckarift, H. R., Spain, J. C., Naik, R. R., & Stone, M. O. (2004). Enzyme immobilization in a biomimetic silica support. *Nature Biotechnology, 22*, 211–213.
13. Du, G. H., Liu, Z. L., Xia, X., Chu, Q., & Zhang, S. M. (2006). Characterization and application of Fe3O4/SiO2 nanocomposites. *Journal of Sol-Gel Science and Technology, 39*, 285–291.
14. Arruebo, M., Fernandez-Pacheco, R., Velasco, B., Marquina, C., Arbiol, J., Irusta, S., Ibarra, M. R., & Santamara, J. (2007). Antibody-Functionalized Hybrid Superparamagnetic Nanoparticles. *Advanced Functional Materials, 17*, 1473–1479.
15. Choi, J., Kim, J., Lee, Y., Kim, I., Parka, Y., & Hur, N. (2007). Fabrication of silica-coated magnetic nanoparticles with highly photoluminescent lanthanide probes. *Chem. Commun.* 1644–1646.
16. Kamelipour, N., Mohsenifar, A., Tabatabaei, M., Rahmani-Cherati, T., Khoshnevisan, K., Allameh, A., Milani, M., Najavand, S., & Etemadikia, B. (2014). Fluorometric determination of paraoxon in human serum using a gold nanoparticle-immobilized organophosphorus hydrolase and coumarin 1 as a competitive inhibitor. *Microchimica Acta, 181*, 239–248.
17. Chou, K. S., & Lee, S. J. (2009). Facile methods to synthesize nanaosized iron oxide colloidal dispersion and its characterization. *Colloids and Surfaces A: Physicochemical and Engineering Aspects, 336*, 23–28.

18. Hashemifard, N., Mohsenifar, A., Ranjbar, B., Allameh, A., Lotfi, A. S., & Etemadikia, B. (2010). Fabrication and kinetic studies of a novel silver nanoparticles-glucose oxidase bioconjugate. *Analytica Chimica Acta, 675*, 181–184.
19. Shanehsaz, M., Mohsenifar, A., Hasannia, S., & Pirooznia, N. (2013). Detection of Helicobacter pylori with a nanobiosensor based on fluorescence resonance energy transfer using CdTe quantum dots. *Microchimica Acta, 180*, 195–202.
20. Zekavati, R., Shahabeddin, S., Hashemi, S. J., Rahmani, T., Tabatabaei, M., Mohsenifar, A., & Bayat, M. (2013). Highly sensitive FRET-based fluorescence immunoassay for aflatoxin B1 using cadmium telluride quantum dots. *Microchimica Acta, 180*, 1217–1223.
21. Lessard-Viger, M., Rioux, M., Rainville, L., & Boudreau, D. (2009). FRET enhancement in multilayer core-shell nanoparticles. *Nano Letters, 9*, 3066–3071.
22. Thakur, S., Kumar, P., Reddy, M., Siddavattam, D., & Paul, A. (2013). Enhancement in sensitivity of fluorescence based assay for organophosphates detection by silica coated silver nanoparticles using organophosphate hydrolase. *Sensors and Actuators B: Chemical, 178*, 458–464.
23. Kim, C., Choi, B., Seo, J., Lim, G., & Cha, H. (2013). Site-specific immobilization of microbes using carbon nanotubes and dielectrophoretic force for microfluidic applications. *Biosensors and Bioelectronics, 41*, 199–204.
24. Sahin, A., Dooley, K., Cropek, D., West, A., & Banta, S. (2011). A dual enzyme electrochemical assay for the detection of organophosphorus compounds using organophosphorus hydrolase and horseradish peroxidase Sensor. *Sensors and Actuators B: Chemical, 158*, 353–360.
25. Pedrosa, V. A., Paliwal, S., Balasubramanian, S., Nepal, D., Davis, V., Wild, J., Ramanculov, E., & Simonian, A. (2010). Enhanced stability of enzyme organophosphate hydrolase interfaced on the carbon nanotubes. *Colloids and Surfaces B, 77*, 69–74.
26. Wang, J., Chen, L., Mulchandani, A., Mulchandani, P., & Chen, W. (1999). Remote biosensor for in-situ monitoring of organophosphate nerve agents. *Electroanalysis, 11*, 866–869.
27. Mulchandani, P., Mulchandani, A., Kaneva, I., & Chen, W. (1999). Biosensor for direct determination of organophosphate nerve agents. 1. Potentiometric enzyme electrode. *Biosensors and Bioelectronics, 14*, 77–85.
28. Roger, K., Wang, Y., Mulchandani, A., Mulchandani, P., & Chen, W. (1999). Organophosphorus hydrolase-based fluorescence assay for organophosphate pesticides. *Biotechnology Progress, 15*, 517–522.
29. Mulchandani, A., Pan, S., & Chen, W. (1999). Fiber-optic biosensor for direct determination of organophosphate nerve agents. *Biotechnology Progress, 15*, 130–134.
30. Mulchandani, P., Mulchandani, A., Chen, W., Wang, J., & Chen, L. (1999). Amperometric thick-film Strip electrodes for monitoring organophosphate nerve agents based on immobilized organophosphorus hydrolase. *Analytical Chemistry, 71*, 2246–2249.
31. White, B., & Harmon, H. (2005). Optical solid-state detection of organophosphates using organophosphate hydrolase. *Biosensors and Bioelectronics, 20*, 1977–1983.
32. Lei, Y., Mulchandani, P., Chen, W., & Mulchandani, A. (2007). Biosensor for direct determinationof fenitrothion and epn using recombinant *Pseudomonas putida* JS444 with surface-expressed organophosphorous hydrolase. *Applied Biochemistry and Biotechnology, 136*, 243–250.